Inverse Dynamics of a Redundantly Actuated Four-Bar Mechanism Using an Optimal Control Formulation

Olavo Luppi Silva
Mechanical Engineering Department,
University of São Paulo,
Av. Prof. Mello Moraes 2231, Butantã,
CEP: 05508-900 -São Paulo-SP, Brazil,
e-mail: olavo.luppi@usp.br

Luciano Luporini Menegaldo[1]
Associate Professor
Mechanical and Materials
Engineering Department,
Military Institute of Engineering-IME,
Praça General Tibúrcio, 80-Praia Vermelha,
CEP: 22290-270-Rio de Janeiro-RJ, Brazil,
e-mail: lmeneg@ime.eb.br

This paper presents an approach to estimating joint torques in a four-bar closed-chain mechanism with prescribed kinematics and redundant actuation, i.e., with more actuators than degrees of freedom. This problem has several applications in industrial robots, machine tools, and biomechanics. The inverse dynamics problem is formulated as an optimal control problem (OCP). The dynamical equations are derived for an open-chain mechanism, what keeps the formulation simple and straightforward. Sets of constraints are explored to force the three-link open-chain to behave as a four-bar mechanism with a crank rotating at a constant velocity. The controls calculated from the OCP are assumed to be the input joint torques. The standard case with one torque actuator is solved and compared to cases with two and three actuators. The case of two actuators presented the smallest peak and mean torques, using one specific set of constraints. Such torques were smaller than the solution obtained using an alternative method existing in literature that solves the redundancy problem by means of the pseudo-inverse matrix. Comparison with inverse dynamics solutions using well-established methods for the one-actuator closed-loop four-bar were equal. Reconstructed kinematical trajectories from forward integration of the closed-loop mechanism with the OCP obtained torques were essentially similar. The results suggest that the adopted procedure is promising, giving solutions with lower torque requirements than the regularly actuated case and redundantly actuated computed with other approaches. The applicability of the method has been shown for the four-bar mechanism. Other classes of redundantly actuated, closed-loop mechanisms could be tested using a similar formulation. However, the numerical parameters of the OCP must be chosen carefully to achieve convergence. [DOI: 10.1115/1.4004064]

1 Introduction

Closed-loop mechanisms comprised of rigid links connected by hinge joints are frequently found in mechanical systems. In some cases, the forces or torques needed to produce a particular movement must be known after the mechanism has been designed or constructed, and the kinematics has been measured. This is the inverse dynamics analysis, which can be performed by well-known methods (for example, that presented by Haug [1]) if the number of degrees of freedom is equal to the number of actuators. Such methods are not straightforwardly applied when the number of actuators is smaller than the number of degrees of freedom, i.e., an *under-actuated mechanism*, or greater, a *redundantly actuated mechanism*. In the second case, there are infinite possible torque solutions that fit the kinematics, and some external *a priori* hypothesis must be introduced to resolve the ambiguity.

One of the methods for resolving such ambiguities is to formulate the *effort-sharing* problem between the actuators as a static optimization. This optimization can be performed by solving a pseudoinverse matrix (see Ref. [2] for theory and Ref. [3] for examples) or by other optimization procedures. In such formulations, the choice of the optimization *objective function* determines, to a great extent, the shape of the torque solution. For the pseudoinverse case, the objective function is the least-squares of the solution vector at every single step. However, the torque found by static optimization will only be optimal for a particular time step and probably not for the entire motion.

Some more sophisticated approaches to solve this problem can be found in the literature, see for example, Nakamura and Ghodoussi [4] and Cheng et al. [3]. By using a Lagrange–D'Alembert formulation, they demonstrated that the dynamic equations of redundantly actuated parallel manipulators (which are actually a class of closed-chain mechanisms) have a form similar to those of a serial manipulator. Equations of motion in terms of the independent generalized coordinates are found, and their right-hand sides are the functions of generalized force or torque vectors. In regularly actuated case, the system of equations is square, while in redundantly actuated one, it is not. The resulting system can be solved by using the Moore–Penrose pseudoinverse matrix [3,5], which minimizes the Euclidean 2-norm of the actuator torques. Ganovski et al. [6] use a different approach, which has been proved to be strictly mathematically equivalent to a pseudoinverse solution. Muller and Maisser [7] extended the pseudoinverse approach in redundantly actuated parallel manipulators to introduce prestress, i.e., internal forces that do not generate end effector wrenches.

Our group have solved the inverse dynamics of the same four-bar mechanism [8] using the Haug [1] formalism. The generalized force terms were changed to include the additional redundant torques, based on a variation of the Valasek transmission matrix [9]. Since the trajectories of the generalized coordinates are known, the resultant system of differential algebraic equations (DAEs) becomes a linear nonsquare system that is solved via the Moore–Penrose pseudoinverse matrix. This solution will be compared in Sec. 4.7 with the results presented here.

[1]Corresponding author.

Contributed by the Dynamic Systems Division of ASME for publication in the Journal of Dynamic Systems, Measurement, and Control. Manuscript received March 6, 2010; final manuscript received March 22, 2011; published online November 11, 2011. Assoc. Editor: Michael A. Demetriou.

This paper presents an alternative formulation, based on optimal control theory, for solving the inverse dynamics of a closed-loop redundantly actuated mechanism. The optimal control variables are the torques that minimize an integral objective function. Mechanism dynamics is fit to a set of constraints, in the sense of optimal control theory: multibody system equations are treated as differential constraints, while closed-loop position equations and the prescribed driving motion are formulated as trajectory algebraic constraints. Actuator saturation limits can also be easily included as control bounds.

This approach has some attractive features. The first is great flexibility in the choice of objective functions: the torques, energies, powers, or any combination of them can be minimized. These choices are not allowed when using the pseudoinverse matrix to solve this problem. Optimality is achieved throughout the entire span of movement, not step-by-step; the latter situation corresponds to solving the left-hand side of the equations of motion from the measured or the calculated kinematics, setting it equal to the sum of moments, and finding the moments through static optimization.

The presented optimal control formulation is reasonably simple and does not require special user skills to write down the equations of the problem, as is the case in the more sophisticated methods cited above. In contrast, there are numerical problems associated with solving the optimal control problem (OCP). The formulation is not unique, and the most suitable *transcription* of the mechanism to the optimal control problem must be determined. Herein, we try to outline some steps to formulate a closed-loop redundant mechanism through optimal control by solving a particular case study, namely, the four-bar mechanism. It is not possible to assert that the same choice of numerical parameters will work for other classes of mechanisms, or what kind of torque patterns could result. However, some useful starting suggestions are provided. The solution of an optimal control problem is a highly problem-dependent task. However, if a particular mechanism can be assumed to be a serial manipulator with a restrained end effector, the approach presented here will be applicable with slight adjustments.

A number of possible problem formulations of the particular case study were tested, considering different numbers of actuators and constraint configurations. The number of actuators is directly related to diverse degrees of actuation redundancy, which are described comparatively. Results suggest that a significant reduction in torque demands can be obtained under one particular set of conditions with two actuators when compared to the single actuator case as well as to the redundantly actuated solution using a classical optimization method.

2 Optimal Control

Optimal control theory offers an interesting perspective on the solution of closed-loop redundantly actuated mechanisms. Different trajectories and controls can be obtained for different choices of the cost function, e.g., minimum torque, minimum torque variations, minimum trajectory deviation from equilibrium, minimum energy etc. When using optimal control to solve the inverse dynamics problem, the trajectory should be introduced in the formulation as a constraint, and different cost functions will result in different control input patterns. The generated kinematic trajectories will be approximately the same if suitable kinematic constraints are formulated. Important aspects related to the kinematics-following accuracy are the constraint violation tolerance of the optimization algorithm and the way in which constraints are formulated within the optimal control problem.

Although optimal control theory has been well-established since the 1960s, its popularity has increased due to the availability of computer packages such as RIOTS [10], MISER3 [11], TOMP [12], and SOCS [13]. Such software packages are able to numerically solve large-scale problems in a straightforward manner, using so-called direct integration methods. The system is formulated as a discretized dynamic optimization problem, and an associated static optimization is solved by off-the-shelf algorithms, such as SQP (sequential quadratic programming). Direct integration methods begin with an initial guess of the control history vectors, numerically integrate the differential equations (e.g., by the Runge–Kutta method) and solve a static optimization problem, resulting in a set of spline coefficients that minimize an augmented cost function accounting for some of the constraints for the entire time of motion.

These methods can address a broad class of highly complex nonlinear problems, which are usually intractable by indirect methods. However, some subtle numerical problems often arise in the discretization and optimization algorithms. The integration-optimization interactions are likely to converge if the control guess is good and if the dynamics integrated with this control does not fall out of the "basin of attraction" of a stable solution. In addition, convergence is easier with a few penalties (i.e., fewer constraints in the formulation) and if the cost function is simpler.

Lee et al. [14] presented an optimal-control-based approach to formulate and solve equations of motion for mechanical systems. It included mechanisms with redundant closed-chains and solved the forward dynamics of the resulting optimal control problem in a numerically efficient way. These authors use a very complex and specific formulation to fit mechanism inverse dynamics into the optimal control problem, based on the theory of Lie groups.

In this paper, a simpler optimal control formulation is proposed to find actuator torques that represent the "*optimal controls*" ($\mathbf{u}^*(t)$) for a prescribed mechanism's kinematics. The MATLAB toolbox RIOTS, developed by Schwartz [15], was used to solve the OCP in the context of *Consistent Approximations Theory*. This software uses a generic formulation of the OCP, offering several numerical algorithms to solve different classes of problems.

The four-bar mechanism was chosen for its simplicity as a case study. Several different formulations were tested using this simple mechanism, to find the most appropriate way to write the constraint equations. In addition, the most suitable numerical algorithms among those available in the RIOTS package were found. Other problems are also addressed by this paper: (i) finding the optimal control torque functions for an exactly actuated closed-loop mechanism (one-actuation, for the four-bar mechanism) and comparing with a classic inverse dynamics analysis to check the solution; (ii) finding the four-bar optimal torques with two and three actuators; (iii) suggesting some OCP formulations and numerical guidelines for solving more complex problems, and (iv) verifying whether the redundantly actuated four-bar mechanism presents smaller maximum torques than the exactly actuated mechanism, allowing smaller actuators in practical applications. Actuator size is an important factor in determining the dynamic performance and payload characteristics of robots powered by redundant actuation systems [5].

3 Methods

3.1 Generic Optimal Control Formulation. A general OCP can be formulated [16–18] to determine the optimal states $\mathbf{x}^*$, the optimal controls $\mathbf{u}^*$, and the final time T (if it is left open) that minimize a cost function G_o [Eq. (1*a*)]. The minimization problem is subjected to the state equations (or dynamic constraints) Eq. (1*b*) that describes the dynamics of the system and various possible additional constraints as required by the problem at hand: initial and final boundary conditions. Eq. (1*c*) and Eq. (1*d*), control upper and lower bounds Eq. (1*e*), and trajectory constraints Eq. (1*f*).

$$\text{min: } G_o(\mathbf{x},\mathbf{u},t) = g_o(\mathbf{x},\mathbf{u},t) + \int_0^T f_o(\mathbf{x}(t),\mathbf{u}(t),t)dt \tag{1a}$$

$$\dot{\mathbf{x}}(t) = \mathbf{f}(\mathbf{x},\mathbf{u},t) \tag{1b}$$

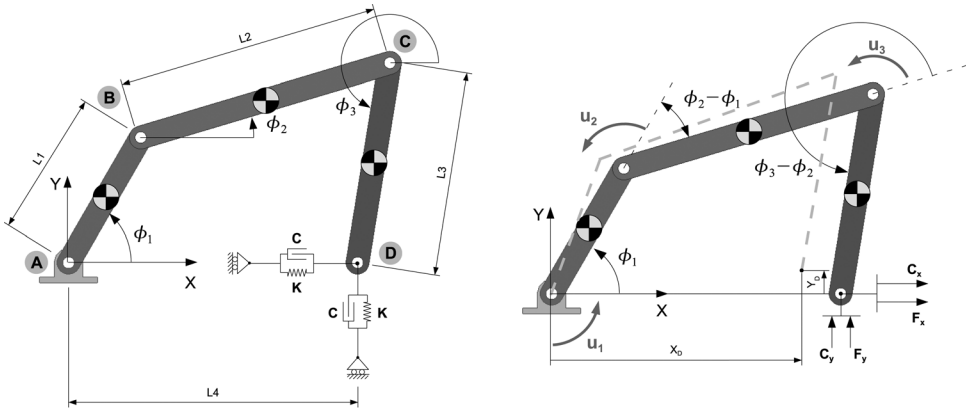

(*a*) Nomenclature and coordinates

(*b*) Control forces, restriction forces and relative coordinates for deduction of generalized force vector

Fig. 1 Dynamical model diagram

$$\mathbf{x}(0) = \mathbf{x}_0 \tag{1c}$$

$$\mathbf{x}(T) = \mathbf{x}_T \tag{1d}$$

$$\mathbf{u}^{min} \leq \mathbf{u}(t) \leq \mathbf{u}^{max} \tag{1e}$$

$$\mathbf{x}^{min} \leq \mathbf{x}(t) \leq \mathbf{x}^{max} \tag{1f}$$

Schwartz and Polak [19] and Polak [20] formulated the OCP as an approximation problem, using Runge–Kutta integration to discretize system dynamics, considering that the initial conditions and an estimation of the control vector are given. A subspace of the discretized control space is used to express the control samples as spline coefficients. Specific formulas were introduced by the authors to guarantee the mathematical equivalence of the internal product and norm operations between the defined functional and the Euclidean spaces. Through these transformations, off-the-shelf static optimization algorithms can be used efficiently to solve the equivalent nonlinear optimization problem.

The algorithms briefly described above were implemented by their authors [10] in the MATLAB Toolbox RIOTS (Recursive Integration Optimal Trajectory Solver). This software allows using first to fourth order fixed step-size Runge-Kutta integrator and first to fourth order splines. The LSODA [21] variable step-size integrator can be also used. The optimization problem is solved with a class of conjugate-gradient techniques [19] or an SQP solver NPSOL [22]. User-defined cost and constraint functions, as well as their symbolic derivatives, are written in ANSI C code and dynamically linked to RIOTS. This paper seeks to address the following question: how can this generic formulation be fit into a multibody, closed-loop, redundant-actuator inverse dynamics problem?

3.2 Dynamical Model. State Eq. (1*b*) are derived from the planar open-chain manipulator equations of motion, with frictionless pin-joints and driven by joint torque actuators. Thus, the closed-loop mechanism is modeled as if it was an open-loop kinematic chain, which derivation is more straightforward. In addition, closed-chain mechanisms require the algebraic position analysis constraints to be solved together with the equations of motion, which leads to a system of DAEs [23]. This class of equations is susceptible to constraint stabilization problems [24,25].

To keep the end effector linked to its support, effectively simulating a four-bar mechanism, external spring and damper forces are introduced at the most distal extremity, as depicted in Fig. 1. If K and/or C are large enough, then external horizontal and vertical reaction forces will keep Point D approximately fixed. Two planar DOFs of the system are mechanically restricted. These elements work as an approximation of the hinge joint that really exists in a four-bar mechanism. They allow for simulation of the weight and dynamic load supporting roles of the joint but retain the multibody equations of the open-chain manipulator. This strategy is frequently used in optimal control studies of human gait [26–28], to model the double-support phase. In this situation, the heel of one foot and the toes of the contralateral one are simultaneously in contact with the ground, forming a closed-loop five-bar mechanism. The contact of the foot to ground is thus modeled as a nonlinear spring and damper.

The left hand side of manipulator equations of motion can be easily derived by means of Lagrange equations [Eq. (2)]. The center of mass positions of each bar are described as a function of the independent angular coordinates φ_j, $j = 1, 2, 3$, as well as the potential and kinetic energies of the whole system

$$\frac{d}{dt}\frac{\partial L}{\partial \dot{\varphi}_j} - \frac{\partial L}{\partial \varphi_j} = Q_j \tag{2}$$

The resulting system of equations takes the form of Eq. (3), where [**A**] is the mass matrix, [**B**] is the centripetal terms matrix, [**C**] is the vector of gravitational terms, [**D**] is a matrix of ones and zeros that relates the torque actuators to the coordinates that they act upon, and [**E**] is a vector that includes the spring and damper forces. The right hand side of Eq. (3) is equal to Q in Eq. (2) and is usually referred to as the "Generalized Force Vector". Different versions of matrix [**D**] are used depending on the case under consideration and are shown in Table 2. Additionally, to be used in the optimal control formulation, Eq. (3) was transformed into state space form

$$\begin{bmatrix} \mathbf{A} \end{bmatrix} \begin{bmatrix} \ddot{\varphi}_1 \\ \ddot{\varphi}_2 \\ \ddot{\varphi}_3 \end{bmatrix} + \begin{bmatrix} \mathbf{B} \end{bmatrix} \begin{bmatrix} \dot{\varphi}_1^2 \\ \dot{\varphi}_2^2 \\ \dot{\varphi}_3^2 \end{bmatrix} + \begin{bmatrix} \mathbf{C} \end{bmatrix} = \begin{bmatrix} \mathbf{D} \end{bmatrix} \begin{bmatrix} u_1 \\ u_2 \\ u_3 \end{bmatrix} + \begin{bmatrix} \mathbf{E} \end{bmatrix} \tag{3}$$

3.3 Specific Optimal Control Formulation. As shown in previous works [29], a careful choice of the objective function and constraints in the formulation of the OCP is important for numerical convergence of the solution. The controls and state-trajectory patterns obtained are also closely related to the chosen

Table 1 Overview of studied cases

		Restricted by	
Number of Actuators	Unrestricted	Spring	Spring + Damper
1	—	Case C	Case D
2	—	—	Case E
3	Case A	Case B	Case F

Table 2 Model parameters and outputs ([*D*]: Eq. (3) matrix; K: Stiffness factor; C: Damping factor; $\delta^D_{\max}$: Point D maximum displacement; $F^D_{\max}$: Point D maximum force; OFV: Objective Function Value; *t*: CPU processing time; OFWP: Objective Function Weighting Parameters, see Eq.(4))

	[**D**]	K (N/m)	C (N.s/m)	δ^D_{max} (m)	F^D_{max} (N)	OF	*t* [min]	OFWP
Case A	$\begin{bmatrix} 1 & -1 & 0 \\ 0 & 1 & -1 \\ 0 & 0 & 1 \end{bmatrix}$	0.00	0.00	$8.95 \cdot 10^{-4}$	0.00	$7.51 \cdot 10^{4}$	46.7	$w_1 = 1$ $w_2 = 1$ $w_3 = 1$
Case B	Idem Case A	$1.00 \cdot 10^{3}$	0.00	$9.50 \cdot 10^{-3}$	$9.50 \cdot 10^{0}$	$4.36 \cdot 10^{4}$	43.9	$w_1 = 1$ $w_2 = 1$ $w_3 = 1$
Case C	$\begin{bmatrix} 1 & 0 & 0 \\ 0 & 0 & 0 \\ 0 & 0 & 0 \end{bmatrix}$	$1.00 \cdot 10^{7}$	0.00	$1.36 \cdot 10^{-4}$	$1.36 \cdot 10^{3}$	—	301.0	$w_1 = 1$ $w_2 = 0$ $w_3 = 0$
Case D	Idem Case C	$5.00 \cdot 10^{6}$	$1.00 \cdot 10^{6}$	$5.22 \cdot 10^{-5}$	$7.82 \cdot 10^{2}$	$9.69 \cdot 10^{3}$	14.3	$w_1 = 1$ $w_2 = 0$ $w_3 = 0$
Case E	$\begin{bmatrix} 1 & -1 & 0 \\ 0 & 1 & 0 \\ 0 & 0 & 0 \end{bmatrix}$	$5.00 \cdot 10^{7}$	$1.00 \cdot 10^{7}$	$5.05 \cdot 10^{-3}$	$7.00 \cdot 10^{2}$	$4.27 \cdot 10^{3}$	67.1	$w_1 = 1$ $w_2 = 1$ $w_3 = 0$
Case F	Idem Case A	$1.00 \cdot 10^{5}$	$1.00 \cdot 10^{4}$	$2.77 \cdot 10^{-3}$	$2.81 \cdot 10^{2}$	$3.34 \cdot 10^{4}$	192.6	$w_1 = 1$ $w_2 = 1$ $w_3 = 1$
Ref. Case	—	—	—	0.00	$7.48 \cdot 10^{21}$	$1.01 \cdot 10^{4}$	0.11	$w_1 = 1$ $w_2 = 0$ $w_3 = 0$

objective function. Herein, the minimization of the sum of squared actuator torques, as shown in Eq. (4), was chosen to be the cost function. By choosing this particular cost function, the Euclidean norm of the torque vector is minimized, although other functions could be proposed. This function has the additional advantage of being convex and simple, which also eases convergence.

Another important issue is the formulation of the OCP constraints. The most noticeable point is that the 3-DOF planar manipulator must comply with the position loop equations of the four-bar mechanism. Different constraint formulations were attempted, for instance making β or γ equal to zero in Eq. (6) but better convergence properties were achieved using $\alpha = 1(\text{adimensional})$, $\beta = 1(\text{s.m}^{-1}.\text{rad}^{-1})$, and $\gamma = 1(\text{s/rad})$. The dimensions of parameters α, β, and γ were set to make Eq. (6) dimensionally consistent. Equations (7*a*)–(7*e*) represent the mechanism position loop equations, their derivatives and an additional equation to make $\dot{\varphi}_1$ constant, imposing a fixed crank angular velocity. Such conditions were transformed into one single trajectory inequality constraint, by squaring and summing all terms into a single equation [Eq. (6)] that must be smaller than a small numerical tolerance *EPSNEQ*. Thus, the specific optimal control formulation for this problem is to find the control vector **u** which minimizes the cost function Eq. (4), subject to equations of motion is state-space form Eq. (5), and the trajectory inequality constraints Eq. (6), whose terms are defined in Eqs. (7*a*)–(7*e*).

$$f(\mathbf{u}) = \int_0^{tf} w_1 u_1^2 + w_2 u_2^2 + w_3 u_3^2 dt \tag{4}$$

subject to

$$\{\dot{\mathbf{x}}\} = \mathbf{g}(\mathbf{x}, \mathbf{u}) \tag{5}$$

$$\alpha^2(f_1^2(\mathbf{x}) + f_2^2(\mathbf{x})) + \beta^2(f_3^2(\mathbf{x}) + f_4^2(\mathbf{x})) + \gamma^2 f_5^2(\mathbf{x}) \leq EPSNEQ \tag{6}$$

where

$$f_1(\mathbf{x}) = L_1\cos(\varphi_1) + L_2\cos(\varphi_2) + L_3\cos(\varphi_3) - L_4 \tag{7a}$$

$$f_2(\mathbf{x}) = L_1\sin(\varphi_1) + L_2\sin(\varphi_2) + L_3\sin(\varphi_3) \tag{7b}$$

$$f_3(\mathbf{x}) = -L_1\dot{\varphi}_1\sin(\varphi_1) - L_2\dot{\varphi}_2\sin(\varphi_2) - L_3\dot{\varphi}_3\sin(\varphi_3) \tag{7c}$$

$$f_4(\mathbf{x}) = -L_1\dot{\varphi}_1\cos(\varphi_1) + L_2\dot{\varphi}_2\cos(\varphi_2) + L_3\dot{\varphi}_3\cos(\varphi_3) \tag{7d}$$

$$f_5(\mathbf{x}) = \dot{\varphi}_1 - 2\pi \tag{7e}$$

The direct integration algorithm requires an initial guess for the control vector, which feeds the state equations to be simultaneously integrated and discretized. It is essential to have a "good quality" [29] initial control guess. If the kinematics resulting from the numerical integrated dynamics, with such control as input, falls into a "basin of attraction" related to a locally stabilizable solution, then the integration-optimization interactions are likely to converge. The solution can escape out of this basin when the constraints, introduced in the cost function as penalties, cause an excessively large update in the optimized control. In some instances, this can lead to a case in which partial solutions, obtained from using wider constraints, are used as the initial guess for the next trial using tighter constraints [29].

One cycle of a four-bar mechanism working in a steady-state regimen was simulated in all trials, with a constant crank angular velocity of 2π rad/s. To complete 1 cycle, it was necessary that $t_f = 1.0(s)$ of simulation, with the following chosen initial conditions: $\varphi_{1_0} = 1.0472(\text{rad})[60.0(^\circ)]$, $\varphi_{2_0} = 0.2907(\text{rad})[16.5(^\circ)]$, $\varphi_{3_0} = 4.5513(\text{rad})[260.7(^\circ)]$, $\dot{\varphi}_{1_0} = 6.2832(\text{rad/s})[360.0(^\circ/\text{s})]$, $\dot{\varphi}_{2_0} = -1.3760(\text{rad/s})[78.8(^\circ/\text{s})]$, and $\dot{\varphi}_{3_0} = 3.4240(\text{rad/s})[196.1(^\circ/\text{s})]$. A medium-size (200 point) time discretization mesh was adopted. The solution to the optimal control problem is represented by a finite dimensional B-spline and has $200 + \rho - 1$ breakpoints (see Ref. [15] for details). Cubic spline interpolation ($\rho = 4$) was used in all cases. The geometric/mass parameters used were $L_1 = 0.5(\text{m})$, $L_2 = 0.9(\text{m})$, $L_3 = 0.7(\text{m})$, $L_4 = 1.0(\text{m})$, $m_1 = 6.59(\text{kg})$, $m_2 = 11.55(\text{kg})$, $m_3 = 9.07(\text{kg})$. The centers of mass were located in the middle of each bar, and their respective moments of inertia were computed by $I = \frac{1}{12}mL^2$. The tolerance EPSNEQ typically varied from 10^{-1} to 10^{-3}.

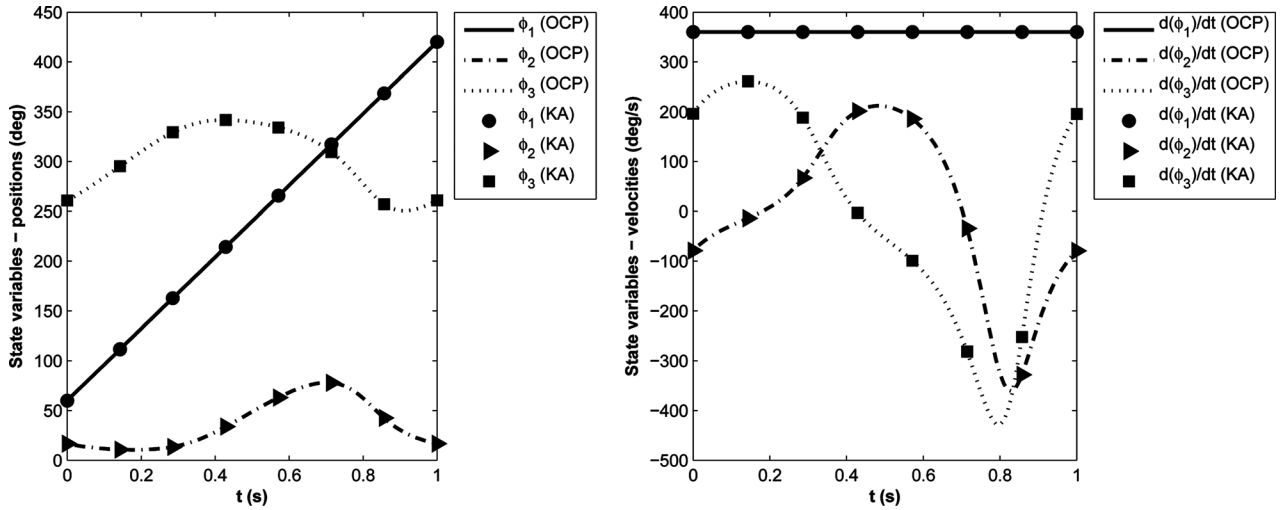

(*a*) Coordinates positions: ϕ_1, ϕ_2, ϕ_3 (*b*) Coordinates velocities: $\dot{\phi}_1, \dot{\phi}_2, \dot{\phi}_3$

Fig. 2 Comparison between optimal control obtained trajectories for case A with kinematic analysis of four-bar mechanism. (OCP: optimal control problem solution, KA: expected trajectory from kinematic analysis).

3.4 Characterization of Studied Cases. Six different configurations of the problem were proposed and can be classified into two main groups: Unrestricted and Restricted. In the Unrestricted group, the manipulator has no force acting on point D, behaving as a moving robotic arm while the end effector keeps still. This case has a limited relationship to four-bar mechanism dynamics and was studied only for numerical testing proposes.

In the restricted group, linear springs or spring and damper reaction forces act to keep point D fixed (in the context of the formulation presented in this paper, the term "restricted" does not refer to a kinematic constraint but to a set of reaction forces caused by a support with large but finite stiffness). The first simulation trials included only the reaction springs, and the dampers were introduced later in an attempt to reduce end-point vibrations observed in the simulations.

As summarized in Table 1, the manipulator has three torque actuators, one for each joint and no restriction forces in case A. In case B, springs are introduced in the horizontal and vertical directions in order to restrict the manipulator. In case C, it remains restricted with springs but with only one actuator at joint A. Case D differs from case C in that a damper force is introduced. The mechanism with two actuators is studied in case E, with springs and dampers. Finally, in case F, three actuators, springs, and dampers are present. The different cases are labeled according to the order in which the simulations were performed. By maintaining this ordering scheme, it is possible to follow the way that simulation parameters were selected to achieve numerical convergence in Sec. 4. The parameters w_1, w_2, w_3 are ones or zeros that fit the objective function into each case studied, as shown in Table 2. The criterion used to choose the "best" solution was based on four aspects, listed in order of importance: (i) RIOTS normal termination; (ii) correspondence between the expected and obtained kinematics, (iii) absence of high torque peaks, and (iv) control curve smoothness.

4 RESULTS

To provide a well-established reference point to compare with the proposed method, a regular kinematic and inverse dynamics analysis was performed [8] for the four-bar mechanism, according to the theory presented by Ref. [1] for a single actuator (Haug case). The trajectories of the angular coordinates and velocities are shown in Figs. 2(*a*) and 2(*b*). All simulations were performed on an Intel Core 2 Duo E6600, 2.40 GHz desktop computer. The associated computational times for each case are shown in Table 2.

4.1 Case A. In case A, the open-chain manipulator with three torque actuators was expected to model the kinematics of a four-bar mechanism, without any mechanical restriction at point D. This situation could be interpreted as the movement of a three-link planar robotic arm in which the first link performs a complete revolution, while its end effector remains fixed. As has already been pointed out, this was not a four-bar linkage and was implemented only for numerical testing.

It was not possible to obtain numerical convergence in a single OCP solution run. Following a strategy used in previous works [29], the gravitational acceleration value was decreased to $g = 4.0(\mathrm{m/s^2})$ in the simulations, and the final time was reduced to $tf = 0.8(\mathrm{s})$(enough time to complete about 80% of the cycle), in an attempt to achieve a normal numerical termination. A vector of zeros was used as the initial guess for the optimal control. The solution obtained with $tf = 0.8(\mathrm{s})$ was used as the initial guess for the next simulation, with $tf = 0.9(\mathrm{s})$. This process was repeated once more, with $tf = 1.0(\mathrm{s})$ and $g = 4.0(\mathrm{m/s^2})$ fixed. Next, the same iterative strategy was used to vary the gravitational acceleration, increasing g by $1.0(\mathrm{m/s^2})$ at time, up to $g = 9.81(\mathrm{m/s^2})$.

The value of *EPSNEQ* is a measure of the violation of the constraint [Eq. (6)] that forces the restricted manipulator to behave as a four-bar mechanism and was initially set to 10^{-3}. A final simulation was performed with $ESPNEQ = 10^{-5}$, in which the solution of a simulation with $ESPNEQ = 10^{-3}$ and $g = 9.81(\mathrm{m/s^2})$ was used as the initial control guess. The state variables trajectories calculated in case A perfectly match the trajectories calculated with regular kinematic analysis of the mechanism, as can be seen in Fig. 2. The error calculated as $\varepsilon = ||OCP_i - KA_i||/||KA_i||$, where OCP and KA refer to the methods and subscript i refers to the state variable, was below 0.002 for all variables.

4.2 Case B. In this case, horizontal and vertical springs were introduced, as shown in Fig. 1(*b*). It should be expected that the inclusion of the spring would play the role of bearing part of the bar weight and should relieve the torque actuators from part of the support against gravity. This hypothesis is confirmed by comparing Figs. 3(*a*) and 3(*b*). The peaks in all torque curves of case B were smaller than in case A, and the value of the objective function in case B was almost 42% smaller than in case A. In fact, the objective function in case A was the highest of all cases studied.

4.3 Case C. In case C, springs were introduced at point D and the restricted manipulator was driven by only one torque

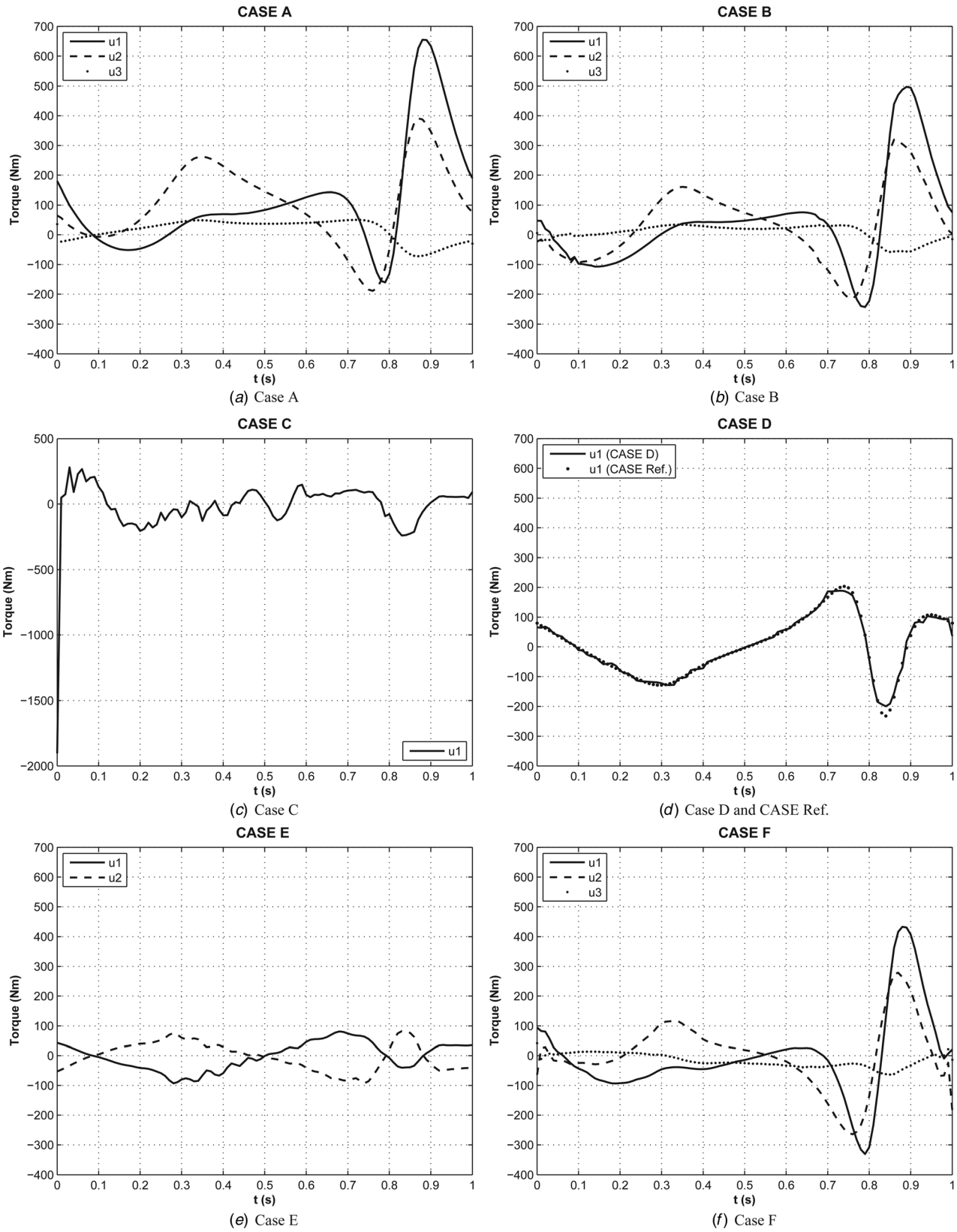

(*a*) Case A (*b*) Case B

(*c*) Case C (*d*) Case D and CASE Ref.

(*e*) Case E (*f*) Case F

Fig. 3 Optimal controls from the best trials of each case

actuator at joint A. With a stiff spring, the behavior of the 3-DOF system is assumed to be approximately that of the closed-loop, 1 DOF four-bar linkage. In this situation, the optimal control solution can be compared to the regular inverse dynamics analysis.

In this case, RIOTS did not converge [Fig. 3(*c*)]. The strategy of starting the simulation sequence with lower gravitational acceleration and smaller final time, as in case A, did not work. The kinematics was reasonably reproduced, but control forces were excessively high.

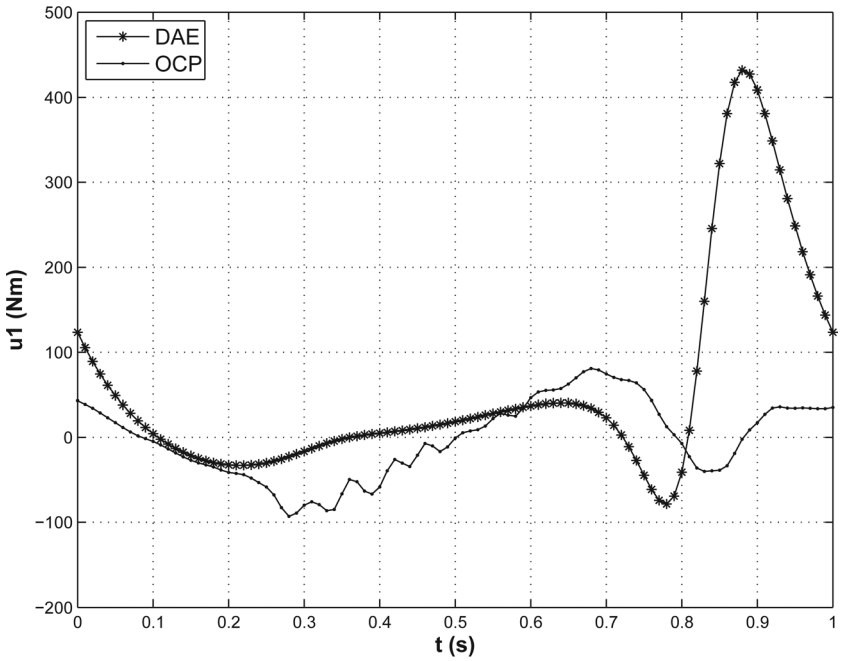

(*a*) Torque on actuator 1

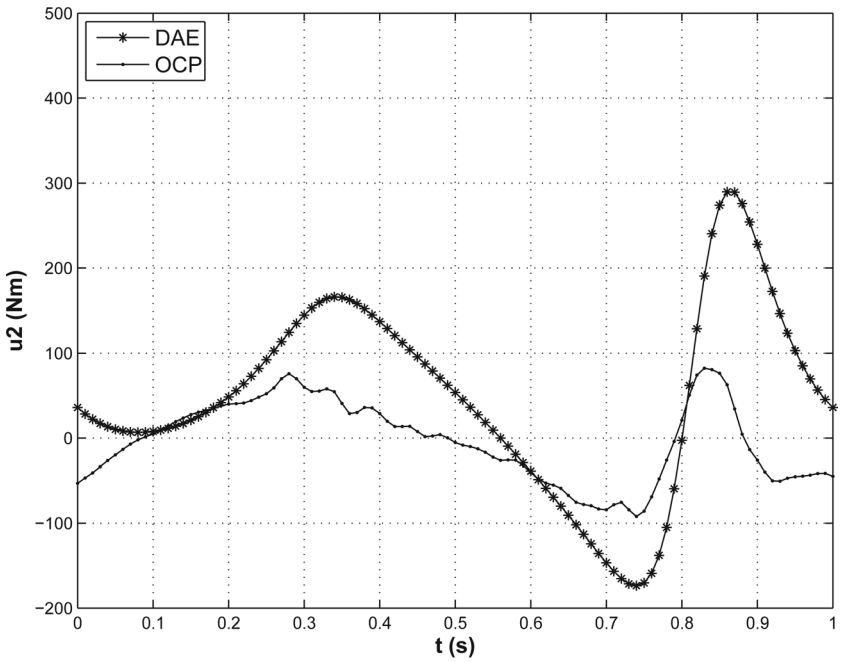

(*b*) Torque on actuator 2

Fig. 4 Torque profiles obtained by a classical solution (DAE) and by proposed optimal control approach (OCP), for case D

4.4 Case D. The experience of case C suggested that the simulations were probably not converging due to the high-frequency excitation force introduced by the undamped spring. Therefore, a damper was introduced in parallel with the springs in case D, and this new element facilitated numerical convergence. By changing the integrator from a fixed step-size fourth-order Runge-Kutta to LSODA (variable step-size, see details in Ref. [10]), successful results could be obtained with a zero initial guess control vector and $tf = 1.0(s)$. Figure 3(*d*) shows that the optimal control solution was similar to the torque calculated by the regular inverse dynamics analysis (Ref. case).

4.5 Case E. The introduction of the spring and damper produced the configuration that best represented a single actuated four-bar mechanism. In case E, this strategy was used with two actuators, at joints A and B. The same successful numerical conditions used in the previous cases were maintained in the first trial of case E, leading to a normal termination, employing the following set of parameters: $g = 9.81(\mathrm{m/s^2})$, $tf = 1.0(\mathrm{s})$, $K = 5.0 \times 10^4$, $C = 1.0 \times 10^4$, $EPSNEQ = 10^{-1}$, the LSODA integrator and a zero initial guess control vector. A smoother curve was obtained using higher stiffness and damping constants (shown in Table 2).

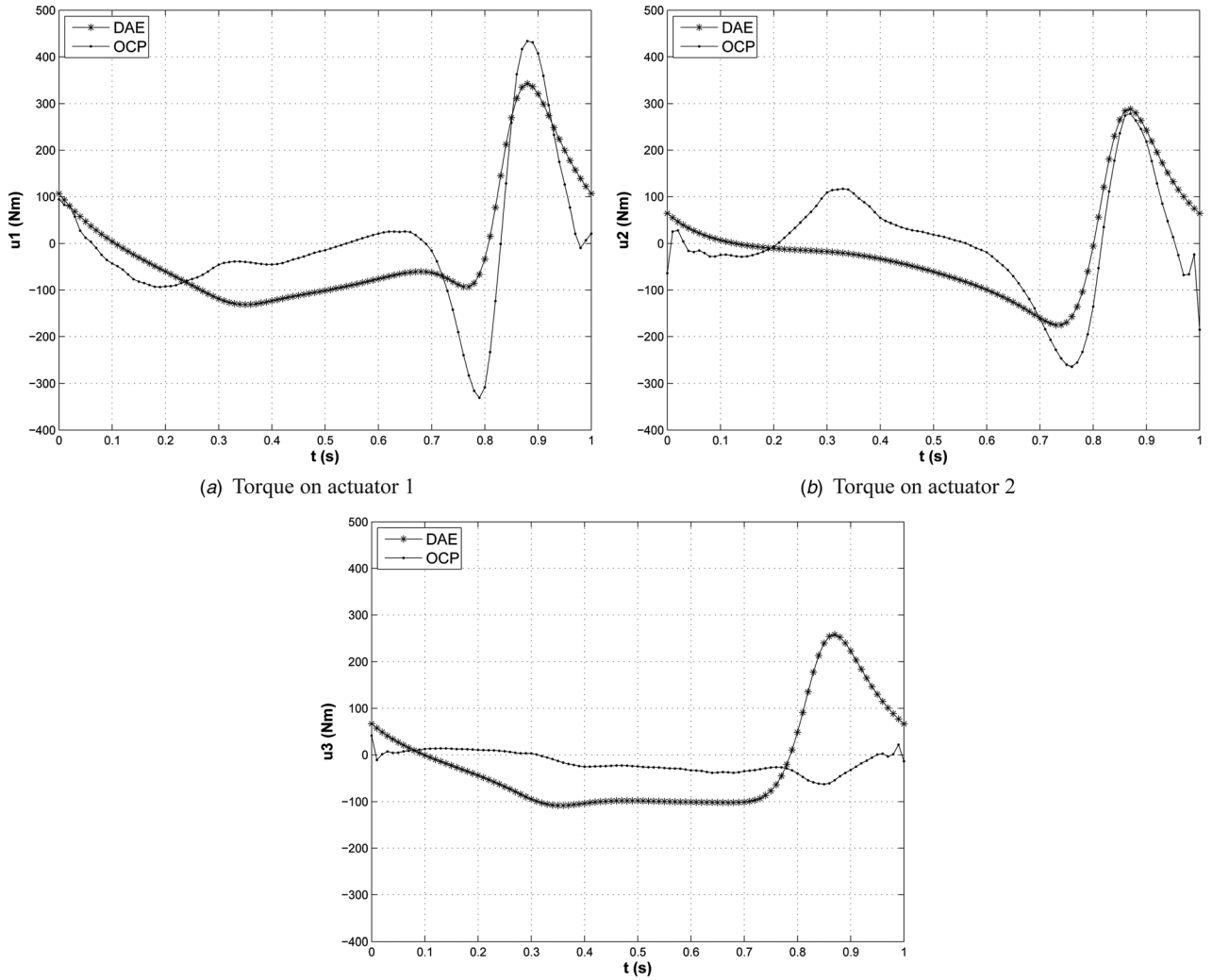

(*a*) Torque on actuator 1

(*b*) Torque on actuator 2

(*c*) Torque on actuator 3

Fig. 5 Torque profiles obtained by a classical solution (DAE) and by proposed optimal control approach (OCP), for case E

Figure 3(*e*) shows that the maximum torque values were significantly smaller than in case D, although their curves were less smooth. This finding is consistent with the objective function value shown in Table 2. It suggests that a four-bar mechanism with two actuators could use smaller motors than the single actuator and obtain the same kinematics.

4.6 Case F. In case F, the three-actuator configuration was revisited, including both the spring and damper that led to good results in cases D and E. Numerical convergence was easily achieved with either a fixed or variable step-size integrator, with no intermediate simulations needed. The torque curves shown in Fig. 3(*f*) were less smooth than cases A and B. However, smaller maximum torques and objective values were obtained than in case B.

4.7 Comparison With a Classical Solution. The same problem has been solved by the authors [8] using a DAE approach. The joint torques for the two- and three-actuator cases are shown in Fig. 4 and 5, respectively. For the three-actuator case, the resulting maximum joint torque requirements are comparable. However, a significant torque reduction was observed in the OCP solution for two actuators.

Table 2 shows the reaction forces and maximum displacements at point D. The reaction forces were calculated by multiplying the displacements and velocities by stiffness and damping values, respectively. The maximum reaction forces were comparable to those obtained in the classical solution. On the other hand, the maximum displacements at point D were not negligible. To verify the extent to which the solutions obtained with the optimal control might diverge from the classical solutions due to such joint displacements, the mechanism dynamics were newly integrated. The control inputs obtained by the optimal control solution were used to drive a forward dynamics simulation in the closed-loop mechanism model (not the three-link manipulator with restrains). A comparison of the trajectories obtained by the OCP solution and those from the integration of the mechanism model with the OCP controls for case D is shown in Fig. 6. This test was repeated for all cases, and similar results were obtained.

5 Discussion

The proposed optimal control approach to solve the four-bar inverse dynamics problem went through the following steps: The first attempt was to control the unrestrained but fixed-endpoint manipulator with three actuators, case A. In case B, a pair of springs in the x and y directions was introduced. In the next step, case C, an attempt was made to force the manipulator to behave as a regular closed-loop four-bar mechanism, with a single actuator, keeping the springs at the endpoint. However, the elastic reaction force made the problem numerically stiff, forcing the

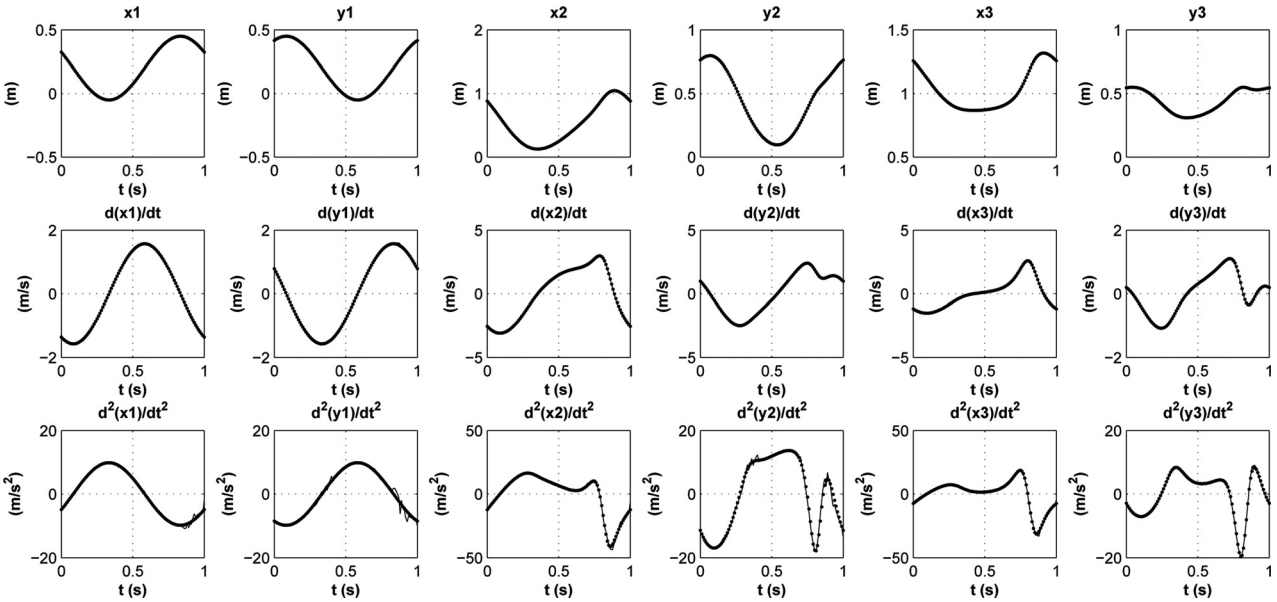

Fig. 6 Cartesian trajectories, velocities and accelerations of joints 1, 2 and 3. Dotted line is OCP trajectory solution from case D, i.e., using the restricted three-link manipulator model. Continuous line is the forward dynamics of the closed-loop four-bar mechanism using optimal control curves from case D as external forces.

fourth-order Runge-Kutta fixed-step numerical integrator to be changed to the variable-step integrator LSODA. In addition, the oscillatory nature of the spring force with no damping produced a nonsmooth control curve. In the next step, case D, a damper was added and the LSODA integrator was used again. This strategy was successful and the resulting control curve matched that obtained using the usual inverse dynamics analysis (Fig. 3(*d*)). Finally, in the last two cases, with two and three actuators—cases E and F, respectively—were explored with the same strategy used in case D.

Some displacement of the bar tip where the spring and damper are connected was observed. However, only marginal differences in the resulting kinematics were observed when the controls were used to drive the classical four-bar closed-loop model, (Fig. 6), especially in the accelerations.

5.1 Objective Function. From Table 2, it is possible to establish a relation between the objective function [Eq. (4)] value and the number of actuators. The six cases studied, listed in order of descending cost function, are: A, B, F, Ref, D, and E. Case C was excluded, since no numerical convergence was achieved. In the first three cases (A, B, and F), the system was driven by three actuators. In case A, the high cost function observed may be attributed to the absence of the support provided by the springs and dampers, since the actuators had to bear all of the weight of the bars. The fourth- and fifth-highest values of the objective function were observed in the cases with only one actuator. Finally, the smallest value was achieved when the system was driven by two actuators, case E.

Table 3 Maximum and minimum actuator torques in a complete crank cycle. Torque values in N.m

	u_1		u_2		u_3	
	max	min	max	min	max	min
Case A	654.7	−160.4	391.1	−188.5	50.3	−72.1
Case B	497.5	−243.2	319.8	−214.9	34.0	−57.5
Case D	188.9	−199.4	—	—	—	—
Case E	80.9	−93.0	82.2	−92.1	—	—
Case F	433.5	−330.9	278.5	−264.4	41.4	−63.3
Ref. Case	203.0	−232.0	—	—	—	—

5.2 Maximum Torque. If the number of actuators increases, is it possible to choose those with smaller maximum torque specifications, which are therefore more lightweight? Table 3 shows the maximum and minimum torques expected from each actuator, for all cases analyzed. Case Ref. shows that it would be necessary to select a motor with a maximum absolute torque greater than 232.0(Nm) for driving the mechanism to perform the prescribed kinematics. When three actuators are used, maximum absolute torque of the most requested actuator is 654.7(Nm) for case A, for 497.5 Nm case B or 433,5 Nm for case F, i.e., two to three times greater than Ref. case.

When using two actuators, the maximum torque was only 93.0(Nm), which is actually less than a half of the maximum reached in case Ref. Thus, the solution of the redundant actuation inverse dynamics problem with the OCP approach has shown that it would be virtually possible to drive this four-bar mechanism using two actuators and using much smaller actuators than the traditional single-actuated case. This result is coherent with Ganovski et al. [6], who also found maximum torque reduction when comparing redundant and nonredundant pick-and-place six-bar planar parallel manipulators. In a real implementation, the existence of motors on the moving links would inevitably alter some of the properties of the links, such as mass and inertia. This effect was not included in the present conceptual study, since actuator specification depends strongly on the particular application of the linkage. In addition, torque could be delivered to the joints, in some cases, by some kind of low-inertia transmission, like belts and chains.

6 Conclusions

An approach to solving the inverse dynamics of a redundantly actuated four-bar mechanism formulated as an optimal control problem has been presented. It permits the closed kinematic chain to be modeled as an open one. However, a pair of high-stiffness virtual springs and dampers should be included at the tip of the chain. Therefore the resulting OCP can be formulated and solved by correctly choosing the appropriate constraint formulation, initial control guess, and numerical algorithms. The most relevant suggestions are including both springs and dampers, using a

variable step-size integration algorithm, appropriate for stiff systems, and writing the OCP constraints as suggested in Sec. 3.3. The main advantage is the relatively easy and straightforward manner in which the dynamical problem can be analytically formulated as an open-loop chain. Optimal control allows for a great deal of flexibility in the formulation of objective functions, hence different torque patterns can therefore be obtained for the same kinematics. In biomechanics, finding the "most physiological" optimization function is a challenging problem, and in the robotic manipulators field, exploring this flexibility is an interesting research topic. It should be emphasized that the solution is optimal throughout the entire time span of the motion, not just in every single step as in static optimization.

Regarding the case of the four-bar mechanism with the specific geometry, mass distribution and kinematics used in this work, it can be stated that using two actuators (case E) presented smaller maximum torques to perform the same kinematical task than its one-actuated (case D) or three-actuated (cases A and B) counterparts. It is not possible to exclude the hypothesis that some optimization solutions corresponded to local minima. This question could be addressed adequately by using hybrid optimization algorithms, which perform a global search, using particle swarm or genetic algorithms, for example, and subsequently a local, more accurate search based on gradient methods [30]. For the nonredundant one-actuator case D, the results obtained through optimal control closely matched those of conventional inverse dynamics analysis.

It does not seem possible to fully generalize the formulation to a very large class of mechanisms without some trial and error work because of the difficulties in selecting the appropriate numerical algorithm, the sequence of simulations to find the initial control guess, and the restriction support characteristics. However, some guidelines have been presented here. Some suggestions for future work include the following: testing the approach in a larger class of mechanisms, such as those with drive singularities, and studying the control patterns that could be obtained with other cost function formulations. This approach is applicable in the biomechanics field, as part of the solution to the muscular actuation redundancy problem in closed-chain systems [31]. Another possible extension of the presented formulation is in considering active actuators at the end chain tip, treating the reaction forces as control variables. It could open interesting perspectives on active control of vibrations in rotating machinery.

Acknowledgment

This research was funded by CAPES—Coordenação de Aperfeioamento de Pessoal de Nível Superior, Brazilian Ministry of Education, CNPq—Conselho Nacional de Desenvolvimento Científico e Tecnológico—Brazilian Ministry of Science and Technology and FAPERJ—Fundação de Amparo à Pesquisa do Estado do Rio de Janeiro.

References

[1] Haug, E., 1989, *Computer Aided Kinematics and Dynamics of Mechanical Systems—Volume 1: Basic Methods*, Allyn and Bacon, MA.
[2] Udwadia, F., and Kalaba, R., 1996, *Analitical Dynamics; A New Approach*, Cambridge University, Cambridge.
[3] Cheng, H., Yiu, Y., and Li, Z., 2003, "Dynamics and Control of Redundantly Actuated Parallel Manipulators," IEEE/ASME Trans. Mechatro., **8**(4), pp. 483–491.
[4] Nakamura, Y., and Ghodoussi, M., 1989, "Dynamics Computation of Closed-Link Robot Mechanisms With Nonredundant and Redundant Actuators," IEEE Trans. Rob. Autom., **5**(3), pp. 294–302.
[5] Lee, Y., Han, Y., Iurascu, C., and Park, F., 2002, "Simulation-Based Actuator Selection for Redundantly Actuated Robot Mechanisms," J. Rob. Syst., **19**(8), pp. 379–390.
[6] Ganovski, L., Fisette, P., and Samin, J., 2004, "Piecewise Overactuation of Parallel Mechanisms Following Singular Trajectories: Modeling, Simulation and Control," Mech. Mach. Theory, **12**(4), pp. 317–343.
[7] Muller, A., and Maisser, P., 2007, "Generation and Application of Prestress in Redundantly Full-Actuated Parallel Manipulators," Multibody Syst. Dyn., **18**(2), pp. 259–275.
[8] Silva, O., and Menegaldo, L., "Inverse Dynamics of a Redundantly Actuated Four–Bar Mechanism Using a Differential Algebraic Equation Approach" , Proceedings of the 20th International Congress of Mechanical Engineering, Gramado-RS, Brazil, edited by ABCM - Brazilian Society of Mechanical Sciences and Engineering, November 15-20.
[9] Valasek, M., Bauma, V., Sika, Z., Belda, K., and Pisa, P., 2005, "Design-By-Optimization and Control of Redundantly Actuated Parallel Kinematics Sliding Star," Multibody Syst. Dyn., **14**(3–4), pp. 251–267.
[10] Schwartz, A. L., and Polak, E., and Chen, Y., "RIOTS Manual—Recursive Integration Optimal Control Trajectory Solver," A MATLAB toolbox for solving optimal control problems, version 1.0 ed. Department of Electrical Engineering and Computer Science, University of California, Berkley.
[11] Jennings, L.S., Fisher, M.E., Teo, K.L., and Goh, C.J., 1991. MISER3: "Solving Optimal Control Problems: an Update", Adv. Eng. Software , Vol. **13**, 190-196.
[12] Kraft, D., 1994, "Algorithm 733: Tomp—Fortran Modules for Optimal Control Calculations," ACM Trans. Math. Softw., **20**(3), pp. 262–281.
[13] Betts, J., Carter, M., and Huffman, W., 1997, "Software for Nonlinear Optimization, Mathematics and Engineering Analysis," Boeing Information and Support Services, The Boeing Company, Library Report mea-lr-83 r1.
[14] Lee, S.-H., Kim, J., Park, F., Kim, M., and Bobrow, J., 2005, "Newton-Type Algorithms for Dynamics-Based Robot Movement Optimization," J. Rob. Syst., **21**(4), pp. 657–667.
[15] Schwartz, A., 1996, "Theory and Implementation of NumericalMethods Based on Runge-Kutta Integration for Solving Optimal Control Problems," Ph.D. thesis, EECS Department, University of California, Berkeley.
[16] Citron, S., 1969, *Elements of Optimal Control*, Holt, Rinehart and Winston, Inc., New York.
[17] Menegaldo, L., 2001, "Modelagem Biomecânica e Controle Ótimo da Postura Humana Através de Algoritmos Baseados na Teoria das Aproximações Consistentes," Ph.D. thesis, University of São Paulo, Sao Paulo, Brazil.
[18] Bottasso, C., Croce, A., Ghezzi, L., and Faure, P., 2004, "On the Solution of Inverse Dynamics and Trajectory Optimization Problems for Multibody Systems," Multibody Syst. Dyn., **120**(1), pp. 1–22.
[19] Schwartz, A. L., and Polak, E., 1997, "Family of Projected Descent Methods for Optimization Problems with Simple Bounds," J. Optim. Theory Appl., **92**(1), pp. 1–31.
[20] Polak, E., 1997, *Optimization: Algorithms and Consistent Approximations*, Springer-Verlag, New York.
[21] Byrne, G., and Hindsmarsh, A., 1987, "Stiff ODE Solvers - A Review of Current and Coming Attractions," Journal of Computational Physics., Vol. **70** pp. 1–62.
[22] Gill, P., Murray, W., Saunders, M., and Wright, M., 1998,. User's Guide for NPSOL 5.0: A FORTRAN Package for Nonlinear Programming. 1998, Systems Optimization Laboratory, Department of Operations Research, Stanford University, Technical Report No. sol 86-2.
[23] Brenan, K., Campbell, S., and Petzold, L., 1989, *Numerical Solution of Initial-Value Problems in Differential-Algebraic Equations*, North-Holland, New York.
[24] Yu, Q., and Chen, I.-M., 2000, "A Direct Violation Correction Method in Numerical Simulation of Constrained Multibody Systems," Comput. Mech., **26**(1), pp. 52–57.
[25] Pennestri, E., and Vita, L., 2004, "Strategies for the Numerical Integration of DAE Systems in Multibody Dynamics," Comput. Appl. Eng. Educ., **12**(2), pp. 106–116.
[26] Yamaguchi, G., and Zajac, F., 1990, "Restoring Unassisted Natural Gait to Paraplegics via Functional Electrical Stimulation: A Computer Simulation Study," IEEE Trans. Biomed. Eng., **37**(9), pp. 886–902.
[27] Anderson, F., and Pandy, M., 1999, "A Dynamic Optimization Solution for Vertical Jumping in Three Dimensions," Comput. Methods Biomech. Biomed. Eng., **2**(3), pp. 201–231.
[28] Anderson, F., and Pandy, M., 2001, "Static and Dynamic Optimization Solutions for Gait are Practically Equivalent," J. Biomech., **34**(2), pp. 153–161.
[29] Menegaldo, L.L., Fleury, A.T., and Weber, H.I., "Optimal control of human posture using algorithms based on consistent approximations theory" In: F. Udwadia, G. Leitmann, and H. I. Weber. (Org.). Dynamical Systems and Control. Boca Raton, FL: CRC Press, 2004, pp. 407–419.
[30] Modares, H., and Sistani, M.-B. N., 2011, "Solving Nonlinear Optimal Control Problems Using a Hybrid ipso-sqp Algorithm," Eng. Applic. Artif. Intell., **24**(3), pp. 476–484.
[31] Menegaldo, L., Fleury, A., and Weber, H., 2006, "A "Cheap" Optimal Control Approach to Estimate Muscle Forces in Musculoskeletal Systems," J. Biomech., **39**(10), pp. 1787–1795.